Thermal Indices for Urban Climate Walk Measurements and Simulations

Peng, Zhikai

Publication date
2024

Document Version
Final published version

Citation (APA)
Peng, Z. (2024). *Thermal Indices for Urban Climate Walk Measurements and Simulations*. Paper presented at CATE 2024 - Comfort At The Extremes, Seville, Spain.

Thermal Indices for Urban Climate Walk Measurements and Simulations

[1,2] Zhikai, Peng
[1] z.p.peng@tudelft.nl, Delft University of Technology, Netherlands
[2] Amsterdam Institute for Advanced Metropolitan Solutions (AMS), Netherlands

Abstract

Thermal variability is essential for assessing outdoor thermal comfort and walkability in urban areas, as it provides thermal-adaptive and alliesthesial opportunities along a walk. This is evidenced by temperature fluctuations that promote passive, intermittent cooling and warming through radiation, convection, and evaporation among buildings, trees, and water bodies. These cooling and warming spots facilitate thermal recovery for pedestrians, as reflected in their metabolic rate, skin and core temperatures, and sweat productions. This paper investigates dynamic thermal comfort along a 3.6 km walk in Rome, Italy, using mobile measurements and simulations (ENVI-met, BIO-met, and Rayman) to explore dynamic thermal indices for forecasting thermophysiological changes due to sun and wind. Two novel thermal indices, $dPET$ and $mPET$, were compared with the static PET maps under non-extreme (September 2021) and extreme (July 2022) weather. The results indicate that both indices capture the temporal progression of environmental and personal parameters. However, they exhibit distinct spatial-temporal patterns owing to their sensitivity to fluctuating thermal conditions. The discussions highlight the need for further lab and field thermophysiological studies to improve dynamic thermal indices for urban climate walk simulations.

Keywords

Thermal indices, Urban Climate Walk, Urban morphology, Dynamic comfort, Thermal alliesthesia

Nomenclature

Abbreviations/Symbols	Descriptions (Units/Scales)
Clo	Clothing level
CWS	Ciampino weather station
EE	Energy expenditure ($kCal/min$)
G	Global radiation (W/m^2)
MET	Metabolic rate (met, or W)
MRT	Mean radiant temperature (°C)
OSM	Open street map
OTC	Outdoor thermal comfort
PET	Physiological equivalent temperature (°C)
RH	Relative humidity (%)
SVF	Sky view factor (0-1)
T_a	Air temperature (°C)
T_{cloth}	Cloth temperature (°C)
T_{core}	Core temperature (°C)
T_g	Globe temperature (°C)
T_{skin}	Skin temperature (°C)
u	Wind speed (m/s)
UCW	Urban climate walk

Introduction: Passive cooling and warming in outdoor spaces

Unlike indoor climates, urban climates are characterised by significant heterogeneity in air temperature, humidity, radiation, and wind. Passive cooling and warming spots can be tactically sequenced through urban design and retrofit focusing on optimising urban shade and breeze. The fundamental mechanisms of passive heat exchange between built environments and their users can be categorised into radiative, convective, and evaporative domains (Table 1).

Table 1: Multiscalar passive cooling and warming opportunities in urban environments

Urban physics	Mitigation at neighbourhood scale	Adaptation at human scale
Radiant-cooling	Building shades, tree shades	Short sleeves, cooling vests, hats
Convective-cooling	Breeze from the park and wind corridor	Inhaling cooler air, cold drinks
Evaporative-cooling	Trees, vegetated walls & roofs, misting	Sweating, swimming
Radiant-warming	Unshaded spaces, beaches	Heavy clothes, scarfs and masks
Convective-warming	Heat exhausts from buildings	Hot showering, hot drinks
Evaporative-warming	Seaside or running rivers in winter	Thermal spring, *onsen*

In summer, pedestrians seek shady and breezy spaces in urban environments to dissipate excess heat gained on unshaded streets, squares, bridges and bus stops, etc. Buildings with heavy thermal mass help stabilise indoor temperatures and cool the streets through radiant cooling, which is particularly effective in alleys and arcades with limited sky exposure and shaded facades. In Rome, small alleys protect pedestrians from direct solar heat, while narrow street canyons enhance convective cooling by channelling winds from various directions (Figure 1). Urban terrain can also twist wind profiles and add vertical flow components at Spanish steps, for example. The stone pines, typically seen in Italian cities provide cooling effects by intercepting direct and reflected short- and long-wave radiations at the canopy level and through evapotranspiration at the leaf level. However, the Tiber River in Rome has a limited capacity to produce a significant cooling or warming effect due to its volume and velocity constraints.

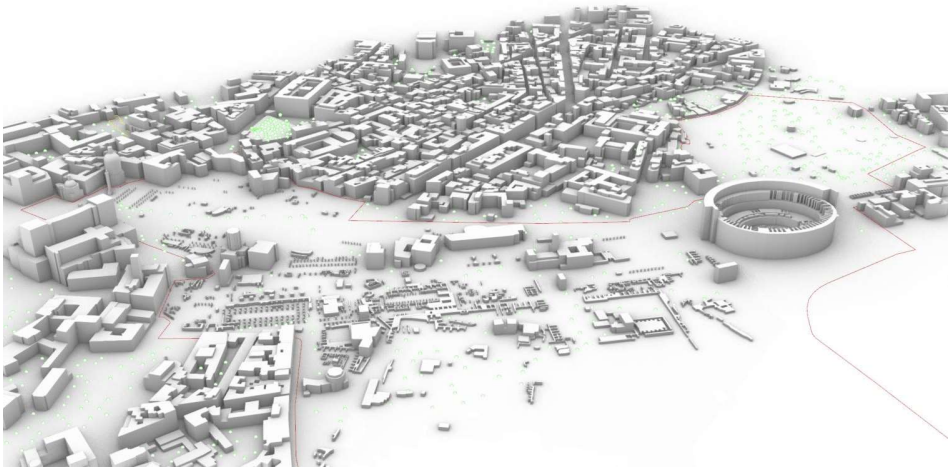

Figure 1: Study area around the Cavour metro station in Rome, Italy

Urban climate walks (UCW) have gained considerable attention in fields of outdoor thermal comfort (OTC) and urban walkability over the past decade. UCW studies aim to understand how pedestrians experience thermal variations shaped by buildings, trees, water bodies, and human activities, and how these thermal contrasts influence their comfort perceptions and spatial behaviours. However, thermal experiences of pedestrians have rarely been examined through a time-series approach, especially concerning their physiological, psychological, and behavioral responses to passive cooling and warming spots across different neighbourhoods, where these thermal-recovery spots play a key role in improving neighbourhood walkability.

Literature Review: Dynamic human thermal comfort

A significant and relatively early work relevant to UCW studies is '*Movement in the Architecture of the City: A Study in Environmental Diversity*' by André Potvin (1997), who conceptualised methods for microclimatic measurements of transients based on sun and wind exposure in Cambridge and Cardiff in the UK. These measurements and urban-analytical methods were later redeveloped and applied across various urban contexts; some incorporated thermal alliesthesia theories (Liu et al., 2021) in hot cities like Phoenix (Dzyuban et al., 2022) and Casbah (Smail et al., 2024), while others combined physiological measurements with questionnaires, as seen in studies conducted in Rome (Vasilikou & Nikolopoulou, 2020; Peng et al., 2022) and Hong Kong (Jiang et al., 2024). Although dynamic OTC research is emerging, many thermophysiological experiments still employ standardised protocols for intermittent cooling and warming with uniformed radiant and convective stimuli outdoors, similar to those used in thermal chambers. This is mainly due to the rigid constraints of physiological experiments, which require stable and controlled boundary thermal conditions that real urban contexts always fail to provide, given the unpredictable weather and anthropogenic activities.

Another expedient approach to studying thermophysiological responses to non-uniformed thermal variations induced by urban morphology is numerical simulations. Most CFD-based software is designed to be deterministic in predicting urban microclimates and static/dynamic OTC across heterogeneous urban fabrics. While not as commonly adopted in thermoregulatory science due to their limited ability to account for uncertainty, sensitivity to small input changes, and challenges with non-linear systems compared to stochastic methods, deterministic OTC software provides useful thermophysiological forecasting for walkability research, particularly for UCW route planning before experiments. Such forecasts require spatial-temporal progression by considering factors like metabolic rate and sweat conditions in various motion states, beyond what can be interpreted from microclimate modelling alone. The virtual demonstrating of dynamic thermal comfort simulation would benefit urban designers, and inform thermal-transitional urban spaces and potential interventions during early-stage design. Subject to reliable validations with ground-truth measurements, numerical simulations of dynamic OTC can guide the design of climate-responsive streets, squares, and parks that are not only protected from thermal extremes but also crafted for thermal allesthesia and pleasure.

This paper investigates dynamic OTC on a 3.6 km walk around Cavour metro station in Rome through mobile measurements and numerical simulations. An exploratory research question is posed: Using OTC software, can current static thermal indices, e.g., PET, be developed into dynamic ones that incorporate thermophysiological forecasting in virtual UCW demonstrations?

Materials and methods

Two workstreams, physical and digital, have been conceptualised to gather and analyse microclimate maps and thermophysiological timeseries data for dynamic OTC assessments. Physical tools listed in Tables 2, 3, and 4 include a mobile weather station, Kestrel Heat Stress Tracker 5400, Ricoh Theta 4 Spherical Camera, and a Fitbit 4 wristband (Figure 2-a) for pulse rate and GPS tracking (Figure 2-b). Additionally, four iButton thermocron sensors (DS1922) were taped on the neck, right scapula, left hand, and right shin for reading skin temperatures. The physical measurements serve as ground-truth references to validate and calibrate digital tools (Figure 2-f), which require morphed weather files (Figure 2-c) and geometry data (Figure 2-d) to define boundary thermal conditions at neighbourhood scale. The digital tools listed in Tables 2, 3, and 4 include the microclimate simulation tool ENVI-met (Figure 2-e) and OTC simulation tools BIO-met (Figure 2-g) and Rayman (Figure 2-h), which integrate static and dynamic thermal indices for visualising dynamic OTC results in 2D and 3D (Figures 2-i, -j).

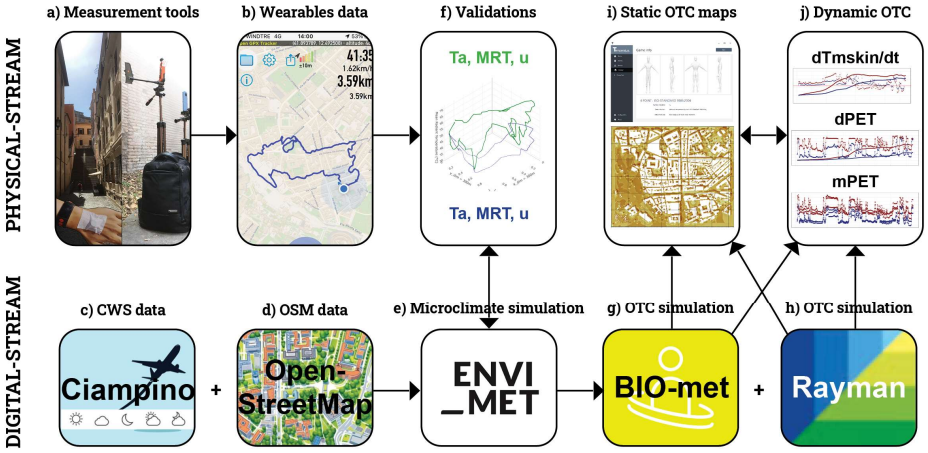

Figure 1: Methodological framework consisting of physical- and digital workstreams for dynamic OTC studies

Weather files were downloaded from Ciampino Weather Station (CWS) and compiled as forcing files for multiple rounds of ENVI-met simulations (850 by 720m) covering two periods: 23–24 September, 2021 (non-extreme period) and 21–22 July, 2022 (extreme period), when the highest heatwave of the decade was recorded for 37°C in air temperature. Each simulation ran from 5:00 am on the first day to 4:59 am on the third day, with data from 1:00 to 2:00 pm on the second day cropped for comparison with measurements. Validation was conducted using the non-extreme period data in 2021 (Diurnal T_a = 20.7 ± 3.0°C, u = 2.7 ± 1.2 m/s), as measurements on extreme heatwave days in 2022 (Diurnal T_a = 29.4 ± 4.6°C, u = 2.6 ± 1.4 m/s) had not been fully launched. The preparation of urban geometrical data, including the meshing (3 by 3 by 3m) of building facades, roofs, pavements, trees, grasses, water bodies, and the terrain factor and telescoping ratio (13% above the highest rooftop), is essential before running the ENVI-met simulation (Table 2). Since information on building materials, tree canopy sizes, and species is largely missing from dati.lazio.it, these details were manually corrected using spherical camera measurements and Google Earth, and then logged in QGIS and Grasshopper.

Table 2: Digital twinning of urban geometry and material data for ENVI-met and Rayman modelling

Urban assemblies	ENVI-met simulation	Rayman simulation	2D/3D GIS data (sizes, heights)	Material attributes (albedo, emissivity)
Facades, roofs, road surfaces, pavements	input	input (not used)	dati.lazio.it	Ricoh camera, Google earth
Trees, grass, water bodies	input	input (not used)	dati.lazio.it (only location data available)	Ricoh camera, Google earth
Topography	input (not used)	input (not used)	dati.lazio.it, OSM	N/A

Metrics

Mean Radiant Temperature (MRT) is a key OTC indicator in UCW assessments, representing the combined effect of all surrounding surface temperatures and radiation on a pedestrian. MRT can be estimated via T_a, T_g and u measurements from the Kestrel 5400 devices (Equation 1).

$$MRT = \left[(T_g + 273.15)^4 + \frac{1.1 \cdot 10^8 \cdot u^{0.6}}{\varepsilon \cdot D^{0.4}}\left(T_g - T_a\right)\right]^{0.25} - 273.15 \quad (1)$$

Where ε and D are the emissivity (0.95) and diameter (0.15m) of the globe, respectively.
In addition to MRT, T_a and u were also used in ENVI-met simulation validation. Wind direction was not chosen for validation due to the greater uncertainty produced by the backpacked Kestrel devices during the UCW measurement. Since both simulation periods were cloudless, the manual forcing of global radiation input was disabled, instead using the solar path module provided by ENVI-met. Other non-atmospheric metrics, such as sky view factor (SVF) and

altitude, were measured but not used as simulation inputs. Therefore, they remain unvalidated in this paper and pending validation in future studies (Table 3).

Table 3: Variables for thermal-environmental measurement and simulation (*indicates measurement data collected but pending validation in future studies).

Physical variables	ENVI-met simulation	BIO-met simulation	Rayman simulation	Measurement/Validation tools
T_a (°C)	input, output	input	input	Kestrel 5400, CWS
RH (%)	input, output	input	input	Kestrel 5400*, CWS
T_g (°C)	N/A	N/A	N/A	Kestrel 5400, CWS
MRT (°C)	output	input	input, output	Equation (1)
u, (m/s)	input, output	input	input	Kestrel 5400*, CWS
Wind direction (deg)	input, output	N/A	N/A	Kestrel 5400*, CWS
G (W/m2) or Cloud cover (0-8)	input	N/A	input	CWS
SVF (0-1)	output	N/A	input	Ricoh spherical camera*
Longitude (deg./min.)	input	N/A	input	Fitbit 4, OSM
Latitude (deg./min.)	input	N/A	input	Fitbit 4, OSM
Altitude (m)	input	N/A	input	Fitbit 4*, OSM
Hour, Day, Year	input	N/A	input	Fitbit 4, CWS

Table 4 presents a part of thermophysiological tools that monitor pulse rates, skin temperatures and provide geolocation data, which are crucial for calculating physiological metrics like BMI, energy expenditure (EE), and metabolic equivalent of workload (MET). BMI is determined through weight and height measurements obtained from a questionnaire, while EE is calculated based on heart rate, weight, age, and gender, with data sourced from Fitbit 4 devices. Physiological validation was not carried in this paper due to insufficient sample size (n = 1).

Table 4: Variables for thermophysiological measurement and simulation in BIO-met and Rayman (*indicates measurement data collected but pending validation in future studies).

Physiological variables	BIO-met simulation	Rayman simulation	Measurement tools
T_{skin} (°C)	output	N/A	iButton thermocrons*
dT_{skin}/dt (°C/min)	output	N/A	iButton thermocrons*
T_{core} (°C)	output	N/A	Ingestive sensors (not used)
T_{cloth} (°C)	output	N/A	Thermal imaging (not used)
MET (met, or W)	input (static), output	input (static), output	Fitbit 4 wrist bands*

Thermal indices

Measurement data were imported into the pythermalcomfort package (Tartarini et al., 2020) to calculate Physiological Equivalent Temperature (PET) under static conditions like standing and sitting. This Python package allows modification of personal variables to compare with ideal indoor climate reference conditions: $T_a = T_g$, wind speed (u) at 0.1 m/s, clothing insulation (clo) at 0.9, and metabolic rate (MET) at 1.37 plus basic metabolism (Equation 2).

$$PET = f(T_a, RH, MRT, u, MET, clo, age, gender, weight, height) \quad (2)$$

ENVI-met enables static PET simulation based on temperature, humidity, radiation, convection around the body, and recently introduced a novel $dPET$ index in the BIO-met module—a dynamic thermal indices that accounts for a constant walking speed, clothing insulation, height, weight, and other factors (Vatani et al., 2024). The personalised inputs reflect changes in T_{core}, T_{skin} and V_{sweat} production along UCW routes, including initial indoor acclimated conditions. The main difference between static PET and $dPET$ is that $dPET$ updates at each time interval along routes, accounting for the 'thermal delay' effect of changing microclimates (Equation 3).

$$dPET(t) = \int_0^T PET(T_{\text{env}}(t), T_{core}(t), T_{skin}(t), T_{cloth}(t), V_{sweat}(t), v_{walking}(t))dt \quad (3)$$

Since the literature for $dPET$ simulation is rare, it remains a black-box approach. So this paper introduces another thermal indices, $mPET$ (Rayman) to benchmark against $dPET$ (ENVI-met)

and the static PET (Rayman + ENVI-met). According the $mPET$ literature (Chen & Matzarakis, 2018), it introduced complex multi-node body and clothing models to predict thermoregulation and heat transfer through convection, radiation, and evaporation, and requires initial skin and clothing temperatures to iterate 1200 times (20 minutes) for heat transfer and energy fluxes between the body, clothing, and surrounding thermal environment (Equation 4).

$$mPET = \frac{1}{1200}\int_0^{1200} PET\left(T_{\text{env}}(t), T_{\text{core}}(t), T_{\text{skin}}(t), \text{Clo}_{\text{multi-layer}}(t), V_{\text{sweat}}(t)\right)dt \quad (4)$$

Based on these assumptions, the final outputs from BIO-met and Rayman ($dPET$ and $mPET$) aim to provide refined estimations of PETs, with $dPET$ depending on a stable speed along a designated walk, and similarly, $mPET$ expected to maintain steady states at all times (Table 5).

Table 5: Simulations of static and dynamic OTC thermal indices

OTC indices	BIO-met simulation	Rayman simulation
PET (°C)	output	output
$dPET$ (°C)	output	N/A
$mPET$ (°C)	N/A	output

Validations

The Root Mean Squared Error (RMSE) results vary between the mobile measurements and ENVI-met simulation results of T_a, MRT and u. See the last page Appendix for more details.

Results: Non-extreme static PET simulation

The static PET map shows that the 3.6 km UCW route covers a range of thermal conditions from 25°C to over 50°C even under non-extreme weathers in 2021. Most cooling spots (dark blue) are located in dense areas on the central, east and north, aligning with building and tree shades. In dense areas, warming spots (dark brown) are often wedged between cooler areas due to direct and reflected solar radiation from the sky and facades, with limited convective-cooling opportunities due to the wind blockage by buildings. Hence, the thermal alliesthesial potential is greater between the warming and cooling spots. To the south and west lies a vast open area with ruins and Roman heritage where the thermal contrasts are less pronounced due to higher wind speeds and reduced variations in intermittent radiant cooling or warming (Figure 3).

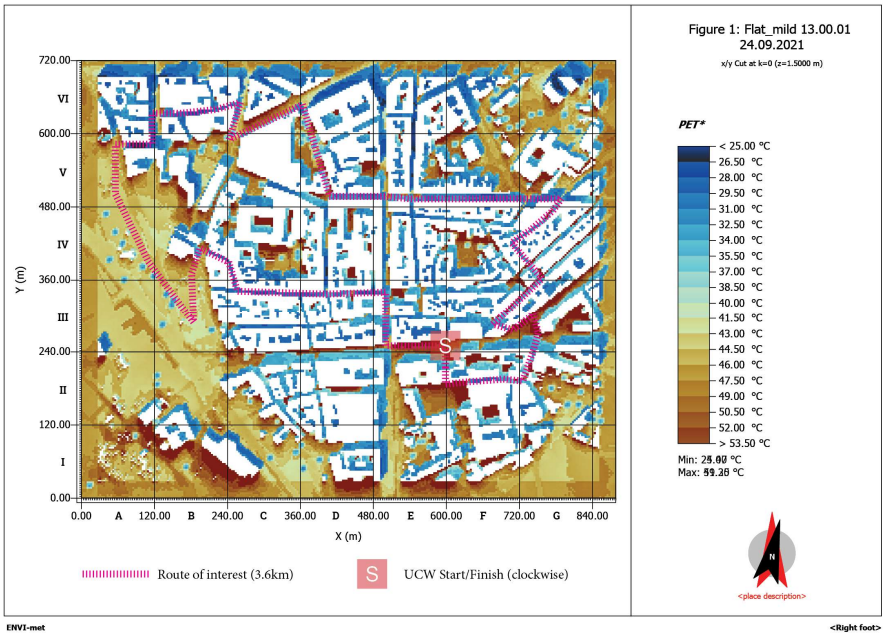

Figure 3: Non-extreme PET map for 24 Sep 2021, 13:00

Results: Extreme static PET simulation

Compared to non-extreme weather in 2021, the extreme scenario in 2022 showed an overall average increase of around 10°C in static PET (Figure 4), with maximum increases up to 32°C around building/tree shades (dark brown), and decreases of -16°C in front of the sunlit facades (dark blue). This suggests that extreme weather can narrow down the PET differences between sun and shade, compromising the intermittent warming and cooling along the UCW routes.

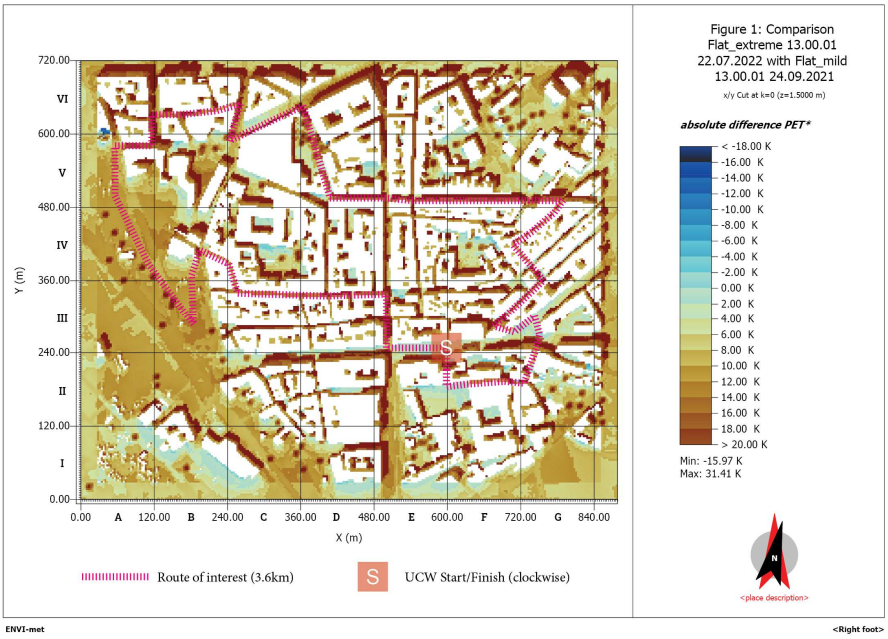

Figure 4: PET comparison between the extreme scenario (22 Jul 2022) and non-extreme (24 Sep 2021) at 13:00

Results: Dynamic OTC simulations

The BIO-met simulations used skin energy balance equations at the skin node to calculate T_{skin}, revealing different rise rates in non-extreme (blue) and extreme (red) scenarios. Both start at a fixed 30°C indoor baseline and increase steadily over the 50-minute simulation (from E-II to G-II geo-coordinates), with peak T_{skin} values reaching 35°C in non-extreme conditions and 37°C in extreme conditions. On the second Y axis, the rate of change of T_{skin}— dT_{skin}/dt (dots) varies more significantly in the second half of the UCW route (from B-VI to G-II geo-coordinates), where the agent navigates sunlit and shaded pavements due to road crossings and turns. Under extreme climate conditions (red), T_{skin} rises and cools more rapidly (±1°C/min) than in non-extreme conditions, suggesting high-risk, high-gain thermophysiological patterns.

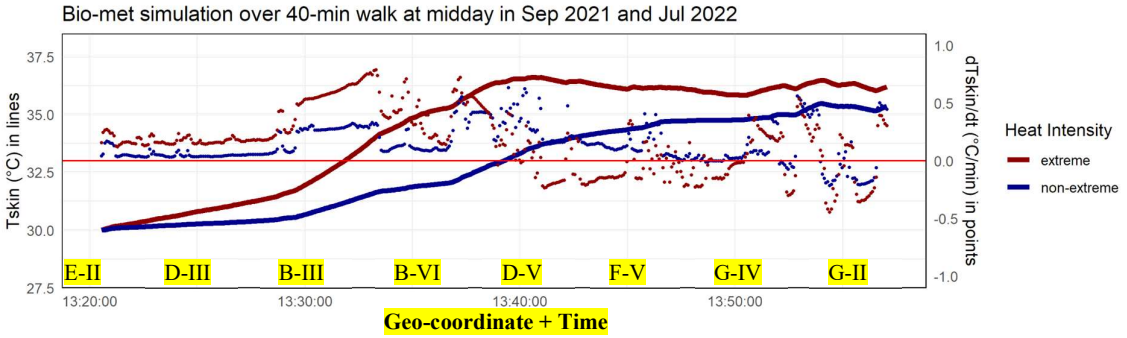

Figure 5: T_{skin}(lines, left Y axis) and dT_{skin}/dt (points, right Y axis) results from the BIO-met simulation. Validation against 4-point mean skin temperature measurements (ISO 9886:2004) is needed in future study.

The simulations of $dPET$ (solid lines) was followed to be compared with the static PET (dots) over the 3.6 km UCW route (Figure 6). Cooling and warming effects from sun, shade, and convective influences are evident in the static PET timeseries. The $dPET$ results (Figure 6) mirrored the T_{skin} simulation (Figure 5), both starting at 20°C under indoor conditions and reaching 32°C in non-extreme scenarios and 45°C in extreme scenarios. However, due to limited literature, it remains unclear why $dPET$ shows a steadier increase than the static PET.

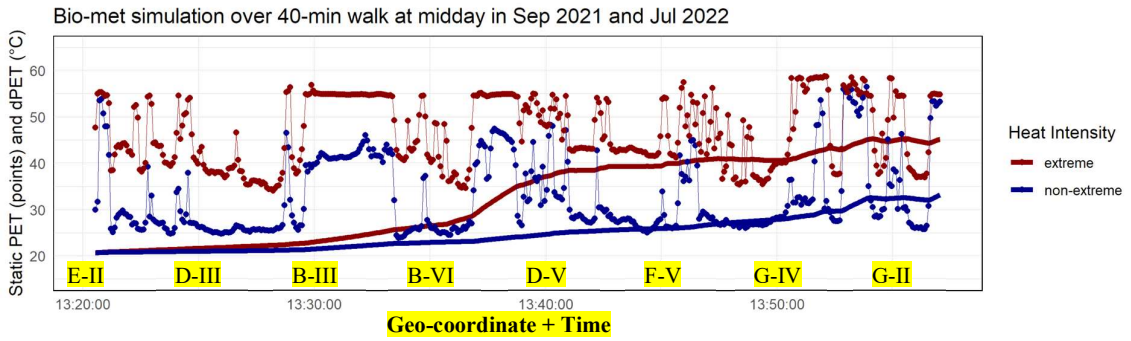

Figure 6: Static PET (dots + lines) and $dPET$ (lines) results from the BIO-met simulation

Figure 7 shows $mPET$ (dots) simulated by Rayman, with patterns distinct from the $dPET$ (solid lines) in Figure 6. The static PET (crosses) simulated by Rayman in Figure 7 also differs from BIO-met in Figure 6, as the static PET (dots) are flattened under extreme weather, which is not observed in Figure 7. In Figure 7, $mPET$ vary from 2°C to 10°C above/under static PET, though their overall fluctuations and turning are quite similar. The gap between $mPET$ and static PET is more pronounced at lower values and under extreme weather conditions. This suggests that $mPET$ predicts more significant intermittent cooling/warming effects than static PET.

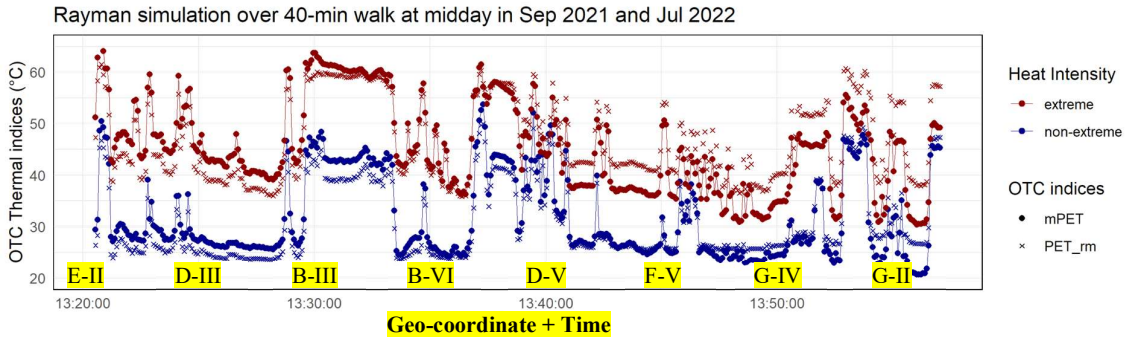

Figure 7: Static PET (crosses) and $mPET$ (dots + lines) results from the Rayman simulation

Discussions and conclusions

The virtual demonstrations of thermal variability along UCW routes could benefit both the OTC and walkability research, as evidenced by the measurements and simulation results. Conditional to successful validation and calibrations, static/dynamic PET visualisations by digital tools such as ENVI-met, BIO-met, and Rayman can forecast thermophysiological variations influenced by diverse meteorological conditions and urban contexts. Importantly, the dynamic UCW simulation is enabled by temporal progression in BIO-met and Rayman, considering increased wind speeds, metabolic rates, and sweat productions. New thermal indices like $dPET$ and $mPET$ can guide decisions in selecting not just 'cool' or 'warm' paths but also 'thermal-alliesthesial' paths. They help in understanding the seasonality and diurnality of thermal alliesthesia and identifies specific times of day or night when pedestrians experience more

pronounced or subtle thermal variations on selected routes. These simulation results can lead to further research into the thermal recovery of skin and core temperatures under extreme weather, where intermittent cooling or warming helps rebalance excessive heat gain or loss, and improve metabolic dysregulation over time—potentially caused by unchanged, chronic heat or cold stress, even if non-extreme (mild), mostly seen in open and unshielded urban areas.

Combining physical and digital tools, this paper has listed existing thermal indices and explore their potential for redevelopment that incorporate built-environmental and thermophysiological parameters. However, this study has limitations. Since dynamic thermal indices have rarely been studied or validated for UCW studies, the conclusions were drawn cautiously, particularly when interpreting and comparing simulation results across different software. This is partly due to the lack of documentation and literature on these new indices. Therefore, the main research question only focuses on the workflows of measurements, simulations, and validation for UCW. Another limitation is the exclusion of topographical effects on urban microclimate, metabolic rate and sweat production. Addressing this would likely require extensive empirical lab and field studies with a sufficient sample size and controlled thermophysiological protocols to develop topographic climate walk models to improve the current dynamic UCW software.

Acknowledgements
This measurement data was collected during my doctoral fieldwork, funded by Department of Architecture and Kettel Yard at University of Cambridge. Thanks to Prof. Minna Sunikka-Blank for inspiring my OTC research in historical urban contexts with a social-technical orientation. The simulation data was prepared during my postdoctoral research funded by the MULTICARE project (101123467). Special thanks to the E&CD Section, AE&T Department, and BK Faculty at TU Delft for supporting conference presentations and travel to CATE 2024.

References
Chen, Y. C., & Matzarakis, A. (2018). Modified physiologically equivalent temperature—Basics and applications for western European climate. *Theoretical and applied climatology*, *132*, 1275-1289.
Dzyuban, Y., Hondula, D. M., Vanos, J. K., Middel, A., Coseo, P. J., Kuras, E. R., & Redman, C. L. (2022). Evidence of alliesthesia during a neighborhood thermal walk in a hot and dry city. *Science of the Total Environment*, *834*, 155294.
Jiang, Y., Xie, Y., & Niu, J. (2024). Short-term dynamic thermal perception and physiological response to step changes between real-life indoor and outdoor environments. *Building and Environment*, *251*, 111223.
Liu, S., Nazarian, N., Hart, M. A., Niu, J., Xie, Y., & de Dear, R. (2021). Dynamic thermal pleasure in outdoor environments-temporal alliesthesia. *Science of The Total Environment*, *771*, 144910.
Peng, Z., Bardhan, R., Ellard, C., & Steemers, K. (2022). Urban climate walk: A stop-and-go assessment of the dynamic thermal sensation and perception in two waterfront districts in Rome, Italy. *Building and Environment*, *221*, 109267.
Potvin, A. J. A. (1997). *Movement in the architecture of the city: a study in environmental diversity* (Doctoral dissertation).
Smail, S. A., Zemmouri, N., Djenane, M., & Nikolopoulou, M. (2024). Investigating the transient conditions of "Sabat" space and its influence on pedestrian sensations during thermal walks. Algiers' Casbah case study. *Building and Environment*, 111760.
Vasilikou, C., & Nikolopoulou, M. (2020). Outdoor thermal comfort for pedestrians in movement: thermal walks in complex urban morphology. *International journal of biometeorology*, *64*, 277-291.
Tartarini, F., & Schiavon, S. (2020). pythermalcomfort: A Python package for thermal comfort research. *SoftwareX*, *12*, 100578.
Vatani, M., Kiani, K., Mahdavinejad, M., & Georgescu, M. (2024). Evaluating the effects of different tree species on enhancing outdoor thermal comfort in a post-industrial landscape. *Environmental Research Letters*, *19*(6), 064051.

Appendix

Note that air temperature (a) and mean radiant temperature (b) results do not include walking scenarios as these two meteorological parameters will not change compared to the standing scenarios. Wind speed (c) and wind directions can change when the subjects move along the trajectories. Wind direction results were excluded due to the unstable conditions of the backpack-mounted Kestrel 5400 while walking. The MRT validation shows the poorest alignment between simulation and measurement, likely due to inaccuracies caused by increased wind speed during the walk, leading to an overestimation in the measured MRT in green (b).

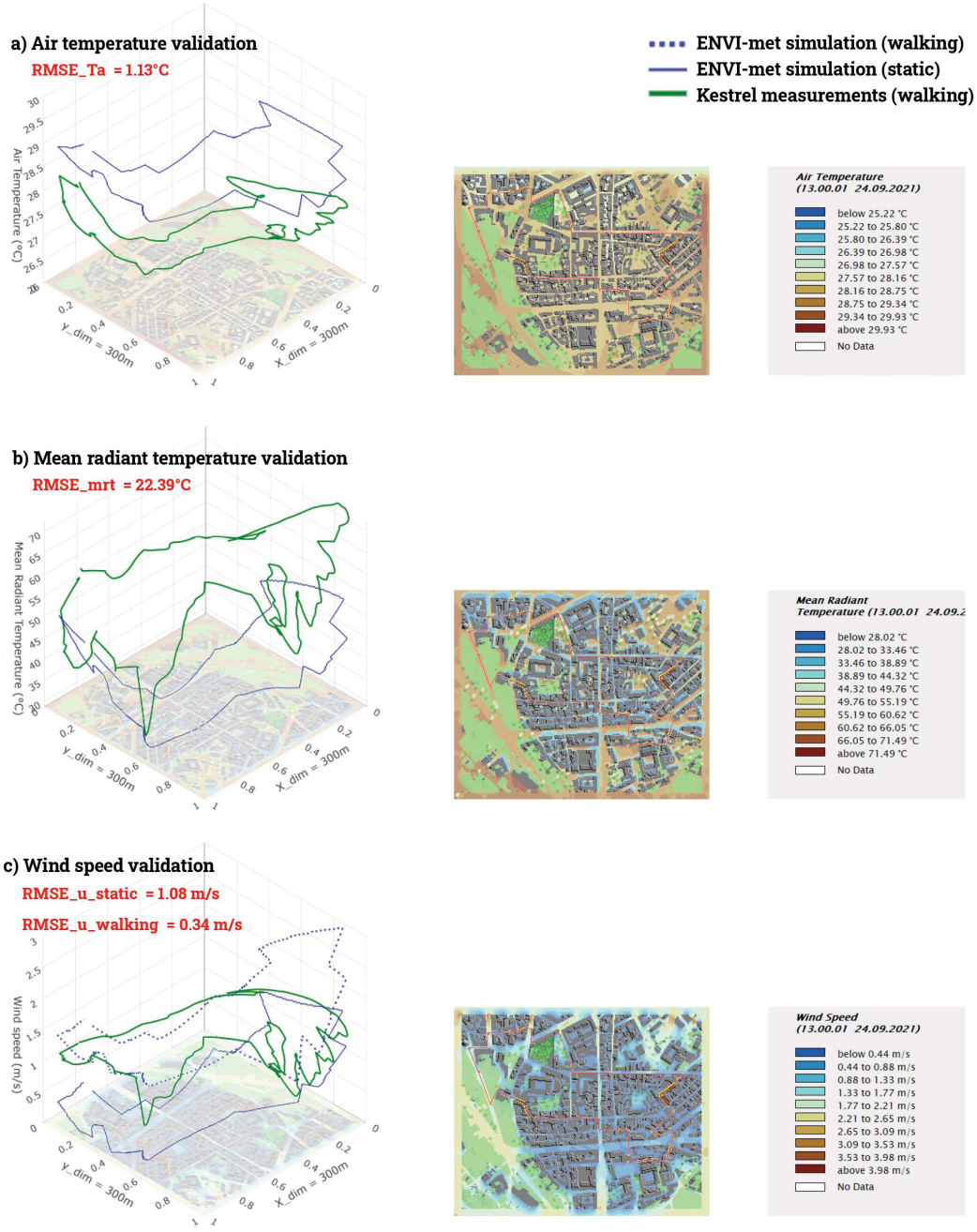

Figure A-1: Validation of air temperature (a), mean radiant temperature (b), and wind speed (c) between ENVI-met simulation and Kestrel mobile measurements on 24 Sep 2021, 13:10 to 14:00.